

Werk

Jahr: 1987

Kollektion: fid.geo

Signatur: 8 Z NAT 2148:61

Digitalisiert: Niedersächsische Staats- und Universitätsbibliothek Göttingen

Werk Id: PPN1015067948_0061

PURL: http://resolver.sub.uni-goettingen.de/purl?PPN1015067948_0061

LOG Id: LOG_0016

LOG Titel: Observation of correlated ULF fluctuations in the geomagnetic field and in the phase path of ionospheric HF soundings

LOG Typ: article

Übergeordnetes Werk

Werk Id: PPN1015067948

PURL: <http://resolver.sub.uni-goettingen.de/purl?PPN1015067948>

OPAC: <http://opac.sub.uni-goettingen.de/DB=1/PPN?PPN=1015067948>

Terms and Conditions

The Goettingen State and University Library provides access to digitized documents strictly for noncommercial educational, research and private purposes and makes no warranty with regard to their use for other purposes. Some of our collections are protected by copyright. Publication and/or broadcast in any form (including electronic) requires prior written permission from the Goettingen State- and University Library.

Each copy of any part of this document must contain these Terms and Conditions. With the usage of the library's online system to access or download a digitized document you accept the Terms and Conditions.

Reproductions of material on the web site may not be made for or donated to other repositories, nor may be further reproduced without written permission from the Goettingen State- and University Library.

For reproduction requests and permissions, please contact us. If citing materials, please give proper attribution of the source.

Contact

Niedersächsische Staats- und Universitätsbibliothek Göttingen
Georg-August-Universität Göttingen
Platz der Göttinger Sieben 1
37073 Göttingen
Germany
Email: gdz@sub.uni-goettingen.de

Observation of correlated ULF fluctuations in the geomagnetic field and in the phase path of ionospheric HF soundings

J. Watermann¹

Institut für Geophysik der Universität Göttingen, Herzberger Landstraße 180, D-3400 Göttingen, Federal Republic of Germany

Abstract. Rapid geomagnetic variations and frequency shifts of ionospherically reflected fixed-frequency continuous radio waves are sometimes closely correlated. Under this aspect, geomagnetic *ssc* and *si* events and *pi2* pulsations recorded between October 1978 and June 1979 at a midlatitude ground station have been studied. About 50% of the *ssc/si*, but only some 30% of the *pi2*, were correlated with radio frequency shifts. In most of these cases the frequency shift can only be interpreted by a vertical motion of the ionospheric *F*-layer. A statistically significant annual variation showing frequent occurrence of correlated events at equinoxes and rare occurrence at solstices has been found. Bivariate complex transfer-function analysis of single events indicates a marked frequency dependence of the relation between radio-wave frequency shifts and variations of the horizontal geomagnetic field. It is estimated to be in the theoretically predicted order of magnitude with smaller daytime values due to a pronounced *E*-layer ionisation and higher integrated conductivities. However, unlike the theoretical expectation, it is found to be approximately frequency proportional in amplitude and randomly distributed in phase.

Key words: Geomagnetic *ssc*, *si* and *pi2* – $\mathbf{E} \times \mathbf{B}$ drift – Vertical ionospheric bulk motion – Transfer functions

Introduction

Time variations of the ionospheric refractive index change the phase velocity of electromagnetic waves and can be observed as phase shifts of high-frequency radio waves. There are two possible mechanisms that can cause the variations: an extraordinary ionisation or recombination of ionospheric particles, or a bulk motion of the charged particles, mainly in the *F*-layer. The first may be due to enhanced UV and X-ray radiation (which is typical for the sunlit side of the earth as a consequence of a strong solar flare effect), or to a solar eclipse; the second can be caused by ionospheric electric fields or neutral air motions. This paper will be restricted to geomagnetic phenomena like *ssc*, *si* and *pi2* events, which are connected with time-varying ionospheric electric fields. In the presence of a non-vertical magnetic field \mathbf{B}_0 it is the vertical component of the $\mathbf{E} \times \mathbf{B}_0$ drift which

forces the electron gas to move up or down. The related radio-wave frequency shift will be called Doppler shift, in accordance with the simplified picture of a wave reflected from a moving mirror. Under certain conditions, observations of the Doppler shift might thus provide some information about the ionospheric electric fields.

Since the IGY 1957/1958, a number of publications have dealt with observations of correlated rapid geomagnetic variations and frequency shifts of fixed-frequency radio waves reflected from the ionospheric *F*-layer (Watts and Davies, 1960; Fenwick and Villard, 1960; Davies et al., 1962; Chan et al., 1962, 1963; Rishbeth and Garriott, 1964; Davies and Baker, 1966; Lewis, 1967; Duffus and Boyd, 1968; Klostermeyer and Röttger, 1976; Menk et al., 1983). But, mainly because of observational inaccuracy and unsuited analysis techniques, no sufficiently concise results could be derived to prove theories quantitatively. In most of the referenced papers, only a qualitative or a classical statistical sample analysis had been carried out. The results suffer from the fact that the physical conditions of the ionosphere might change remarkably even within an hour, which makes the common comparative statistics quite uncertain.

In this study, ground-based observations of geomagnetic and radio frequency variations have been analysed using a time-series regression technique for each individual event. It turned out that it was more adequate to analyse the Fourier-transformed time series instead of the time series themselves. Therefore, not the common regression method in the time domain but its more general counterpart in the frequency domain is preferred. This means that, for every single event, complex coefficients of the relation between the Doppler shift and a combination of the orthogonal horizontal magnetic field variations are estimated at separated frequencies in a least-squares sense. Such a set of coefficients is named a transfer function. It shows the relation in different frequency bands at the same time, i.e. under the same geophysical conditions. The general tendency seen in the transfer functions of all individual events indicates how to interpret the whole sample.

Instrumentation and field observations

After preliminary observations in the winter 1977/1978, the main campaign of simultaneous geomagnetic and ionospheric observations lasted from October 1978 until the end of June 1979, but with interruptions during the winter and spring seasons.

¹ Present address: Herzberg Institute of Astrophysics, National Research Council of Canada, Ottawa, Ontario, Canada K1A 0R6

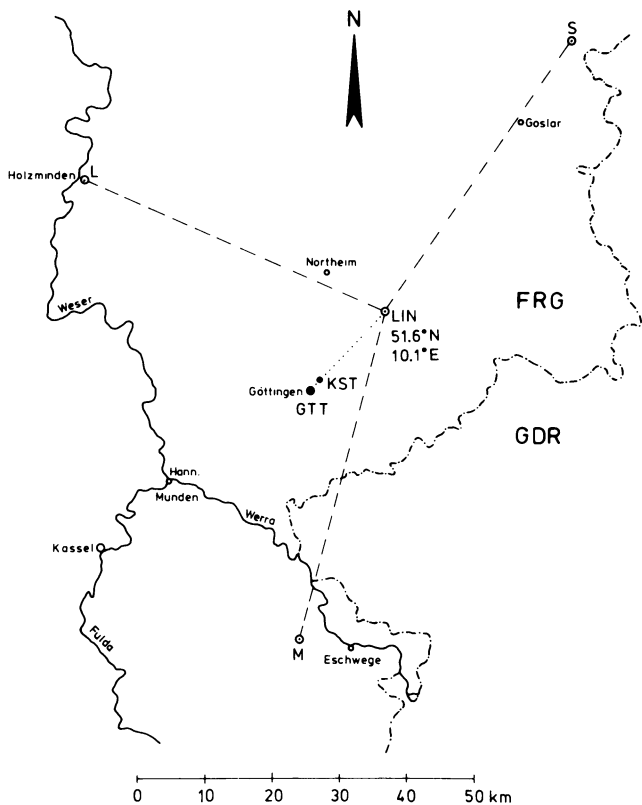


Fig. 1. Observation facilities: *GTT* and *KST* are locations of the ground-based three-component magnetometer, *L*, *M* and *S* are those of the three HF-CW radio transmitters, and *LIN* is the common receiver. Some geographic details are added for orientation

With the help of a three-component search coil magnetometer in combination with an electronic amplifier and low-pass filter device, geomagnetic fluctuations in the period range from 4 s up to some thousand seconds were observed. Together with accurate quartz-clock time information, they were recorded on magnetic tape in an automatically working low-power digital data-acquisition system with a 12-bit analog-to-digital converter. The sampling rate was 30 readings per minute in each component. Until December 1978, the magnetometer was set up in a forest near Göttingen (symbol *KST*), and in March, April and June 1979 it was placed close to the Geophysical Institute of Göttingen University (*GTT*).

At the same time, high-frequency continuous radio waves were emitted at three stations in the vicinity of Göttingen, named Mönchhof (*M*), Schladen (*S*) and Holzminden (*L*). The Doppler shifts of the signals reflected in the ionosphere were recorded at the Max-Planck-Institut für Aeronomie (MPAe) in Lindau (*LIN*). They were transformed to voltage variations and fed into a data-acquisition system identical to the above-mentioned one. The transmitters worked at frequencies 4.5885 MHz, 4.5890 MHz, and 4.5900 MHz, respectively. They were stable enough to allow frequency shifts of 0.1 Hz to be resolved in the time scale of interest (4–1000 s). The HF system is part of the MPAe-SOUSY technical equipment and is described in detail by Röttger and Becker (1977) under the name HF-CW-Doppler radar.

A comparison with data from the MPAe ionosonde showed that for all nighttime events analysed in this study

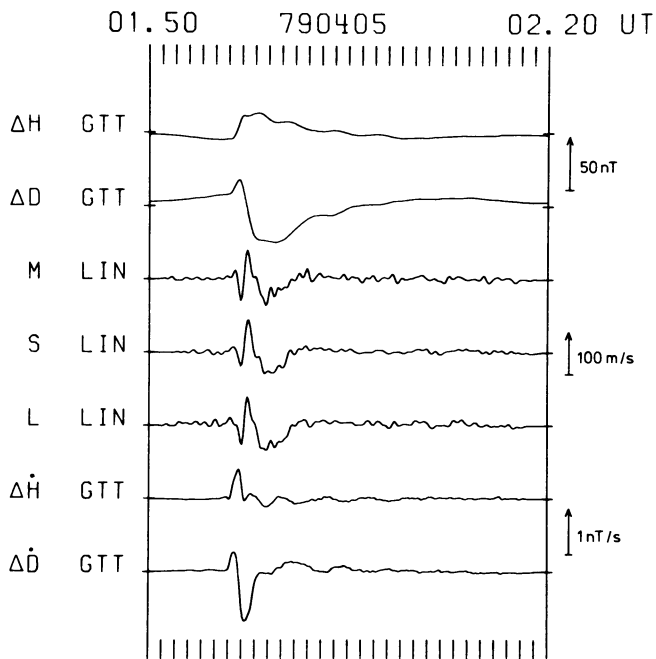


Fig. 2. The *ssc* of April 5, 1979. From top to bottom: time series of the geomagnetic northward and eastward components, ΔH and ΔD , the phase height variations of the three HF signals emitted at stations *M*, *S* and *L*, and the time derivatives of ΔH and ΔD . Scaling bars at the right, minute marks at the top and bottom, and the beginning and end of the time interval in UT

the radio waves had been reflected at virtual heights h' between 210 km and 450 km. As the distance between transmitter and receiver was 50 km on average, the special case of almost vertical incidence was realised.

A geographic orientation is presented in Fig. 1. It shows that the three radio-wave reflection points were roughly straight above the geomagnetic observation point, a situation that is different from most of those in previous publications.

As an example, Fig. 2 shows the recording of the *ssc* on April 5, 1979. From top to bottom, the horizontal magnetic field variations in the northward and eastward direction, ΔH and ΔD , the phase height variations (which are the frequency-shift variations multiplied by a constant factor – see next section) of the three radio signals, *M*, *S* and *L*, and the time derivatives of the magnetic field variations are to be seen. The short vertical lines at the lower and upper margin mark integer minutes, and the beginning and end of the interval in UT are written above.

Theoretical aspects

Let $n(s)$ be the ionospheric refractive index along a ray path S , ψ the angle between the ray direction (direction of energy transport) and the wave normal (which is zero in an isotropic ionosphere), f_0 the frequency of the emitted radio wave and c_0 the vacuum light velocity. A time variation of the refractive index results in a wave frequency shift of Δf at the receiver:

$$\Delta f = -\frac{f_0}{c_0} \frac{dP}{dt} \quad (1)$$

with

$$P = \int_s n(s) \cos \psi ds \quad (2)$$

denoting the phase path.

In the case of vertical incidence, the phase path only depends on the reflection height h_0 , irrespective of the geometry of the ray path. Defining the phase height h_p by

$$h_p = \int_0^{h_0} n(h) dh \quad (3)$$

it can be shown that $P = 2h_p$. For midlatitude regions and frequencies of about 4.6 MHz, only the real part $\mu(h)$ of the refractive index is of significance. Although the geomagnetic field influences the refractive index, only electron density variations and not magnetic field variations themselves have a directly observable effect on the phase height variations. Introducing the magneto-ionic parameters $X = \omega_p^2/\omega_0^2$, $Y = \omega_e/\omega_0$, and $Z = v_e/\omega_0$, (with the radio-wave angular frequency ω_0 , the squared plasma frequency $\omega_p^2 = e^2 N_e/\epsilon_0 m_e$, the electron gyrofrequency $\omega_e = e B_0/m_e$ and the effective electron collision frequency v_e), we get

$$\Delta f = -\frac{2f_0}{c_0} \frac{d}{dt} \int_0^{h_0} \mu(h, t) dh \approx -\frac{2f_0}{c_0} \int_0^{h_0} \frac{\partial \mu(X, Y)}{\partial X} \frac{\partial X(h)}{\partial t} dh. \quad (4)$$

Let us first consider a simple physical model. If we assume a horizontally stratified ionosphere with height-integrated Pedersen and Hall conductivities Σ_P and Σ_H , and an ionospheric height-independent electric field \mathbf{E} that drives a horizontal sheet current density \mathbf{j} in the E -layer, we can map the electric field along the field lines up to the F -layer and will find a Hall drift \mathbf{v} of the electrons

$$\mathbf{v} = \frac{\mathbf{E} \times \mathbf{B}_0}{B_0^2} = \frac{(\Sigma^{-1} \cdot \mathbf{j}) \times \mathbf{B}_0}{B_0^2} \quad (5)$$

with Σ denoting the height-integrated conductivity tensor. If we assume a bulk motion of the F -layer with velocity \mathbf{v} and no significant effect of the lower ionosphere on a radio wave reflected in the F -layer, we find the vertical component v_z of \mathbf{v} to be equal to the time derivative of h_p (e.g. Davies et al., 1962):

$$\frac{dh_p}{dt} = v_z. \quad (6)$$

Neglecting damping effects in the lower atmosphere (which are only valid for variations of short scale compared to the E -layer height) as well as induction effects in the earth, we can calculate the ground magnetic field produced by the sheet current density. Its northward and eastward components, ΔH and ΔD , are related to the radio-wave frequency shift Δf by

$$\Delta f(t) = -\frac{2f_0}{c_0} \frac{2 \cos I}{\mu_0 B_0 (\Sigma_P^2 + \Sigma_H^2)} [\Sigma_P \Delta H(t) + \sin I \Sigma_H \Delta D(t)] \quad (7)$$

where I denotes the magnetic inclination. Electromagnetic induction in the earth changes the horizontal magnetic field only by a factor of between 1 and 2, which is not much compared to the variability of the ionospheric parameters.

The basic ideas of this Hall drift model have been formulated by Rishbeth and Garriott (1964); for details of the calculations see Watermann (1984).

In a refined model, developed by Jacobs and Watanabe (1966) and extended by Watermann (1984), the vertical component of the electron drifts is evaluated along the whole phase path in the ionosphere. It varies with height, as the electron mobility in the lower ionosphere is influenced more by collisions. Although the electron drift differs from a pure $\mathbf{E} \times \mathbf{B}_0$ drift, it can be shown that in a typical average state of the ionosphere the particle drift above about 200 km height is almost unaffected by collisions. At every fixed height along the phase path, the vertical component of the electron drift is observed as a local electron density variation. If electron enhancing processes like solar flare effects are neglected and if the electron density relaxation time is long compared with the period of the electron density variation, one arrives after some algebra at a frequency shift Δf related to a "mean" phase height velocity \bar{v}_z :

$$\Delta f = -\frac{2f_0}{c_0} \bar{v}_z \quad (8)$$

with

$$\begin{aligned} \bar{v}_z &= \gamma_0 (J_N E_N + J_E E_E) \\ \gamma_0 &= e^2 / (4\pi^2 f_0^2 m_e \epsilon_0) \end{aligned} \quad (9)$$

$$J_{N,E} \approx -\int_0^{h_0} \frac{\partial \mu}{\partial X} \frac{\partial}{\partial h} (N_e b_{N,E}) dh$$

$$\begin{aligned} b_N &\approx \frac{\cot I}{B_0} \frac{(v_i - i\omega)\omega_i}{(v_i - i\omega)^2 + \omega_i^2} \\ b_E &\approx \frac{\cos I}{B_0} \frac{\omega_i^2}{(v_i - i\omega)^2 + \omega_i^2}. \end{aligned} \quad (10)$$

ω_i denotes the ion gyrofrequency and v_i the ion-neutral collision frequency. If a height-integrated current density \mathbf{j} is related to the height-independent electric field \mathbf{E} by the height-integrated conductivity tensor Σ [see Eq. (5)], one observes magnetic field components ΔH and ΔD on the ground related to \bar{v}_z by

$$\begin{aligned} \bar{v}_z &= \frac{\gamma_1}{\Sigma_P^2 + \Sigma_H^2} [(\sin I J_N \Sigma_H + J_E \Sigma_P) \Delta H \\ &\quad + (-\sin^2 I J_N \Sigma_P + \sin I J_E \Sigma_H) \Delta D] \end{aligned} \quad (11)$$

with

$$\gamma_1 = \frac{e^2 c_0^2}{2\pi^2 f_0^2 m_e}.$$

In this paper, electron density variation periods of more than 15 s (angular frequencies $\omega < 0.4 \text{ s}^{-1}$) are studied. Compared to $\omega_i > 150 \text{ s}^{-1}$ in the central European geomagnetic field, b_E remains nearly independent of ω , and b_N varies with ω only where ω becomes comparable to v_i . That requires a radar reflection height of more than 300 km, which is higher than that of most of the observed events examined for this paper. Even for the radar signals which were reflected in that high region, the effect of ω is weak. Above ~ 300 km, we find $|\partial(N_e b_N)/\partial z| \ll |\partial(N_e b_E)/\partial z|$. If that height contributes substantially to the integrals $J_{N,E}$, one

sees that $|J_N| \ll |J_E|$, and \bar{v}_z is not much influenced by ω . The physical background is provided by the fact that the charged particle drift is nearly $\mathbf{E} \times \mathbf{B}_0$ oriented at this height, and \bar{v}_z is mainly determined by the east-west electric field E_E , as \mathbf{B}_0 is inclined to the north. In this model, the Hall drift plays the important role. Probably of more interest than $\omega \gtrsim v_i$ is the case $\omega \ll v_i$, as can be seen from what follows where the Alfvén wave model is examined.

In the case of Alfvén waves propagating downwards onto an ionosphere with uniformly distributed integrated conductivity, the electric fields of the incident and the reflected waves superpose. Pedersen currents and field-aligned currents form a solenoid current system with no remarkable magnetic field on the ground, where only the magnetic field of the Hall current is observable [see Glaßmeier (1984) and references therein]. Thus, the Alfvén wave model of Rishbeth and Garriott (1964), neglecting ionospheric modification of the magnetic fields, no longer holds in that formulation. But we can set $\Sigma_p = 0$, and Eq. (11) will be simplified

$$\bar{v}_z = \frac{\gamma_1 \sin I}{\Sigma_H} (J_N \Delta H + J_E \Delta D). \quad (12)$$

The electric field of Alfvén waves is established by a small difference between the motions of electrons and ions. Therefore, the electron velocity \mathbf{v} is close to the ion velocity \mathbf{v}_i , and both are almost equal to the centre-of-mass velocity. The momentum equation for a fully ionized quasi-neutral plasma can be applied to an ionized gas, embedded in the neutral gas of the ionosphere, if an ion-neutral collision term ν_i , damping the ion motion, is included:

$$\frac{\partial \mathbf{v}_i}{\partial t} = -i\omega \mathbf{v}_i = -\frac{1}{\mu_0 \rho_i} \mathbf{B}_0 \times \text{rot } \Delta \mathbf{B} - \nu_i \mathbf{v}_i. \quad (13)$$

$\rho_i = N_e(m_e + m_i) \approx N_e m_i$ denotes the mass density of the ionized gas component. Now, Eq. (12) has to be replaced by

$$\bar{v}_z = \frac{\gamma_1 \sin I}{\Sigma_H} (J_N \Delta H + J_E \Delta D) (1 + i\nu_i/\omega)^{-\frac{1}{2}}. \quad (14)$$

If $\nu_i/\omega > 2$, an approximation with an error of less than 6% reads:

$$|(1 + i\nu_i/\omega)^{-\frac{1}{2}}| \approx (\omega/\nu_i)^{\frac{1}{2}}. \quad (15)$$

In the present study, only angular frequencies less than 0.4 s^{-1} are regarded. Thus the approximation (15) can be used at least up to about 250 km, and even throughout the F -layer for the lower frequencies.

For a quantitative calculation, besides the integrated conductivity, some information about the undisturbed electron density profile $N_e(h)$ and the collision frequency $\nu_i(h)$ is required, while $\partial \mu / \partial X$ can easily be calculated from the Appleton-Hartree equation. ω_i is well known and changes very little with time. If no observations are available one has to use model ionospheres to get the order of $J_{N,E}$. It turns out from numerical calculations that there is not much difference between the values of the coefficients in the models described by Eq. (7) and Eqs. (8)–(11), as the main contribution to the phase path variation stems from the drift of the more dense electron gas in the F -layer above the current sheet.

Neglecting a possible modification with frequency according to Eq. (14), both models show that the observed quantities $\Delta f(t)$, $\Delta H(t)$ and $\Delta D(t)$ should follow the bivariate regression model

$$\Delta f(t) = -\frac{2f_0}{c_0} [h_H \Delta H(t) + h_D \Delta D(t) + \delta(t)] \quad (16)$$

with a noise (or random) term $\delta(t)$ added. Inspection of the observed time series suggests that it is adequate to regard the noise as present mainly in the output Δf of the model.

It should be noted that both regression coefficients h_H and h_D are positive in both models if evaluated with reasonable ionospheric parameters. The coefficients become larger with smaller integrated conductivities. They vary between $h_H \approx 0.3$, $h_D \approx 0.6 \text{ m nT}^{-1} \text{ s}^{-1}$ at noon and $h_H \approx 20$, $h_D \approx 30 \text{ m nT}^{-1} \text{ s}^{-1}$ at night. For all numerical calculations, a magnetic inclination of 67° , a total field strength of 48000 nT and the model ionospheres proposed by Gurevich (1978), which are valid for midlatitude regions and moderate solar activity, have been used.

Occurrence of correlated events

During the time of simultaneous observations, 8 *ssc*, 10 *si*, and 137 *pi2* occurred. Three *ssc* and seven *si* were daytime events. The distinction between day and night that will extend throughout the analysis is defined by sunrise and sunset at a height of 120 km above the ground, which is roughly the height of the maximum electron production rate by solar radiation.

All *pi2* events with onsets within 30 min were combined to a group event. Firstly, it seems reasonable (in contrast to the single-event analysis in the next section) to study the statistics of groups as the midlatitude ionosphere is assumed not to change too much during half an hour; secondly, ionosonde data were only available in 1-h intervals. Of the resulting 115 groups, 41 had to be excluded from the analysis because of a too poor signal-to-noise ratio in the radar signal records. Of the remaining 74 groups, 19 occurred during daytime.

All *ssc*, but only half of the *si*, could be recognized by their Doppler shifts, and these were nighttime and high-amplitude daytime events. Only one-third (26 out of 74) of the *pi2* could be identified in the Doppler data, without a statistically significant difference between day and night. The same holds for the variability with geomagnetic activity or E -layer critical frequency: no significant dependence on these parameters could be found.

But a striking result was a rather frequent occurrence of correlated *pi2* events around the equinoxes and a rare occurrence at the solstices, as can be seen from Table 1

Table 1

Observation interval	Number of <i>pi2</i> groups		Probability of randomness
	Correlated	Total	
02.10.–04.11.78	7	20	18.5%
09.11.–09.12.78	3	15	9.9%
08.03.–13.04.79	14	22	0.1%
12.06.–01.07.79	1	17	0.3%

The last two lines in Table 1 show a deviation from the total distribution which could be drawn randomly only by a probability of 0.1% and 0.3%, which means that the deviation is regarded as significant.

Data analysis and interpretation

In this section the 49 correlated, more or less worldwide geomagnetic events (8 *ssc*, 5 *si*, and 26 *pi2* groups comprising 36 single *pi2*), will be studied individually. An analysis on the basis of the regression model, Eq. (16), shows that the regression coefficient estimates h_H and h_D are in general clearly larger for nighttime than for daytime events. This was expected from the daily variation of the integrated conductivity. The absolute values of h_H and h_D are of comparable size and vary between about 1 and 5 m nT⁻¹ s⁻¹ in daytime and 3 and 25 m nT⁻¹ s⁻¹ at night. But, the regression coefficients have both positive and negative signs which seem to be randomly distributed.

A look back to Fig. 2 indicates that the discrepancy might be due to the use of a simple time-domain regression analysis, while the relation between Δf and ΔH or ΔD seems to be highly frequency dependent. The same holds for the other analysed events. Therefore, the analysis was repeated in the frequency domain with the Fourier transforms $\Delta \tilde{f}(\omega)$, $\Delta \tilde{H}(\omega)$ and $\Delta \tilde{D}(\omega)$ of the original time series. The regression model Eq. (16) is then superseded by the transfer-function model

$$\Delta \tilde{f}(\omega) = -\frac{2f_0}{c_0} [G_H(\omega) \Delta \tilde{H}(\omega) + G_D(\omega) \Delta \tilde{D}(\omega) + \delta(\omega)] \quad (17)$$

of which Eq. (16) is only the special case of frequency-independent transfer functions G_H and G_D .

For each individual event, $G_H(\omega)$ and $G_D(\omega)$ were estimated by means of smoothed Fourier products under the condition that the residuum $\langle \delta(\omega) \delta^*(\omega) \rangle$ is a minimum. The smoothing procedure used a Papoulis window (Papoulis, 1973) of frequency-dependent bandwidth. The number of Fourier products inside the spectral windows varied between 5 and 50. As not all of the three radio signals could be used for the analysis all of the time because of technical trouble, it was only sometimes possible to average the Fourier products over three estimates, and sometimes over two, and sometimes not at all. Therefore, the degrees of freedom and confidence limits of the transfer function estimates were different for different events and different frequency bands.

All estimates of G_H and G_D and their upper 90% confidence limits show a tendency to increase with frequency, while most of the lower 90% confidence limits are near zero. As an example, Fig. 3 shows the upper confidence limits of G_H (left panel) and G_D (right panel) of the analysed *ssc* and *si* events on a logarithmic scale. The *ssc* are marked by integers and the *si* by capital letters, with solid lines for nighttime and dashed lines for daytime events. In the upper part, the central frequencies and bandwidths of the smoothing windows are drawn. A similar picture (not shown here) with the same numerical scale holds for the *pi2* events. There is no general difference between the behaviour of *ssc*/*si* and *pi2* but there is a clear difference between day and night for both of them. The daytime and the nighttime values appear like realisations of two different bell-shape-distributed random processes. Therefore, the estimates of all daytime transfer functions on one hand and

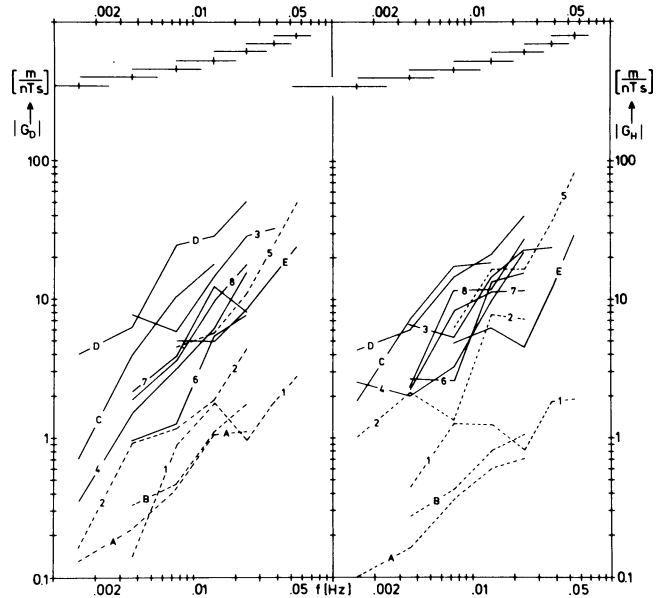


Fig. 3. Upper 90% confidence limits of the absolute transfer-function values of the investigated *ssc* (marked by integers) and *si* (capital letters). Daytime events with dashed lines, nighttime events with solid lines. Right panel for the geomagnetic northward, left panel for the eastward component. Frequency bands with central frequencies and overlapping bandwidths are indicated in the upper part

of all nighttime transfer functions on the other are combined in Fig. 4. It shows the means and standard deviations of the logarithms of the absolute values (lower panel) and the phases (upper panel) of the transfer functions.

In every quadruple the lines have the following meaning: dashed lines with triangles (extreme left) represent the daytime estimates of G_D , dashed lines with open circles (extreme right) represent those of G_H . The solid lines are of similar meaning but for nighttime events: on the left with triangles are the estimates of G_D , and on the right with open circles are those of G_H . The triangles and circles mark the mean values, and the lengths of the lines represent the range of the standard deviations. The short lines at the lower margin indicate the central frequencies of the different bands, while the broad solid bars at the right and left margin of the phase panel give the theoretical standard deviation of randomly distributed phases. The conclusions that can be drawn from Fig. 4 are:

1) The absolute values of the northward and eastward magnetic field components do not show a significant difference in their relation to the phase height variations.

2) With the exception of the lowest frequency band, the transfer function estimates of nighttime events are larger by a factor of about 4 compared to the daytime estimates.

3) There is no indication of a decrease with increasing frequency above 0.01 Hz, unlike Duffus and Boyd (1968) stated.

4) The geometric means of the absolute values of the transfer functions are roughly frequency proportional. The dotted interrupted line which has a gradient of 0.5 on a logarithmic scale (equivalent to a square-root relation on a linear scale) shows a frequency dependence according to Eq. (14) with approximation (15), and would be expected from the results of Klostermeyer and Röttger (1976). Obviously, it does not match the observations. Furthermore,

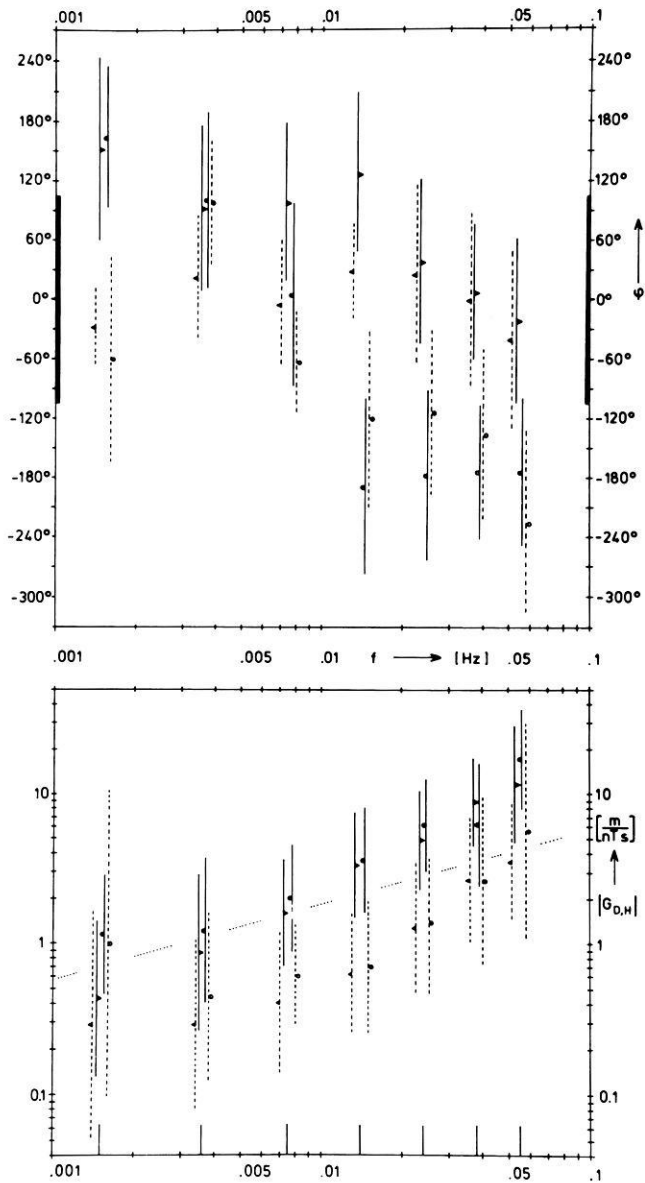


Fig. 4. Mean values and standard deviations of the logarithms of the absolute values and of the phases of all transfer functions. Daytime events with *dashed lines*, nighttime events with *solid lines*. For further explanations see the text

the gradient should become smaller with increasing frequency while Fig. 4 indicates just the opposite: the gradient tends to increase, i.e. the growth rate of the transfer function tends to be higher with higher frequencies.

5) The mean values of the phases do not show a clear daily variation but a difference in the magnetic east and north components. For higher frequencies, \bar{v}_z and ΔD are nearly in phase, and \bar{v}_z and ΔH are nearly in opposite phase. But as the standard deviations of the phase are not much smaller than those of a random uniform distribution, the phases have only little meaning.

Conclusions

As all time-varying magnetic fields observed on the ground must be accompanied by electric fields, and as the lower

atmosphere is a very bad conductor (i.e. its skin depth is several magnitudes larger than its height extension up to the ionospheric *E*- and *F*-layer), there should be an accompanying ionospheric electron drift with a vertical component in midlatitude regions. By the method of observing phase path variations of reflected HF-radio signals described above, the electron drift could not always be detected. Because of this result and the fact that several parameters, mainly the vertical profiles of electron density and collision frequencies or integrated conductivities, are necessary for exact calculations of the electric field, this simple and easy-to-use method does not seem to be sufficiently accurate for calculating the ionospheric electric fields. But the results can be used to find an answer to the question of whether the relation between the frequency of the field variations and the vertical bulk motions of the electron gas is square-root like, linear or quadratic in general. From the results presented here a linear relationship is favoured, which means that none of the presented models will, without major revisions, be supported by the observations. It should be stressed that this relationship comes from averaging single-event spectra, i.e. it is independent of time variations of ionospheric parameters.

Lastly, one must remember that some unsolved questions remain: for example the marked annual variation of correlated occurrence, or the fact that so many geomagnetic events could not be detected by phase shifts, or the nearly randomly distributed phases.

Acknowledgements. This paper is based on the author's doctoral thesis prepared at the Institut für Geophysik der Universität Göttingen. The steady support of Professors M. Siebert and U. Schmucker is acknowledged. The study was only possible with the help of data provided by the Max-Planck-Institut für Aeronomie (Katlenburg-Lindau). The kind support of the SOUSY-group members, especially Dr. J. Röttger, Dr. J. Klostermeyer, E. Prager and H. Becker, is gratefully acknowledged.

References

- Chan, K.L., Kanellakos, P., Villard, O.G. Jr.: Correlation of short-period fluctuations of the earth's magnetic field and instantaneous frequency measurements. *J. Geophys. Res.* **67**, 2066–2072, 1962
- Davies, K., Baker, D.M.: On frequency variations of ionospherically propagated HF radio signals. *Radio Sci.* **1** (5), 545–556, 1966
- Davies, K., Watts, J.M., Zacharisen, D.H.: A study of F2-layer effects as observed with a Doppler technique. *J. Geophys. Res.* **67**(2), 601–609, 1962
- Duffus, H.J., Boyd, G.M.: The association between ULF geomagnetic fluctuations and Doppler ionospheric observations. *J. Atmos. Terr. Phys.* **30**, 481–496, 1968
- Fenwick, R.C., Villard, O.G. Jr.: Continuous recordings of the frequency variation of the WWV-20 signal after propagation over a 4000-km path. *J. Geophys. Res.* **65**(10), 3249–3260, 1960
- Glaßmeier, K.H.: On the influence of ionospheres with non-uniform conductivity distribution on hydromagnetic waves. *J. Geophys.* **54**, 125–137, 1984
- Gurevich, A.V.: Nonlinear phenomena in the ionosphere, *Physics and Chemistry in Space Vol. 10*. New York – Heidelberg – Berlin: Springer-Verlag 1978
- Jacobs, J.A., Watanabe, T.: Doppler frequency changes in radio waves propagating through a moving ionosphere. *Radio Sci.* **1**(3), 257–264, 1966
- Klostermeyer, J., Röttger, J.: Simultaneous geomagnetic and ionospheric oscillations caused by hydromagnetic waves. *Planet. Space Sci.* **24**, 1065–1071, 1976

- Lewis, T.J.: The association of phase changes of ionosphere-propagating radio waves and geomagnetic variations. *Can. J. Phys.* **45**, 1549–1563, 1967
- Menk, F.W., Cole, K.D., Devlin, J.C.: Associated geomagnetic and ionospheric variations. *Planet. Space Sci.* **31**(5), 569–572, 1983
- Papoulis, A.: Minimum-bias windows for high-resolution spectral estimates. *IEEE Trans. Inform. Theory* **IT-19**(1), 9–12, 1973
- Rishbeth, H., Garriott, O.K.: Relationship between simultaneous geomagnetic and ionospheric oscillations. *Radio Sci. J. Res. NBS* **68D**(3), 339–343, 1964
- Röttger, J., Becker, H.: Die HF-CW-Dopplermethode und ihre Anwendung in der Ionosphärenforschung. *Kleinheubacher Berichte* **20**, 243–254, 1977
- Watermann, J.: Beobachtung korrelierter ULF-Fluktuationen im erdmagnetischen Feld und im Phasenweg ionosphärischer HF-Sondierungen. *Diss. Math.-Nat.-FB, Univ. Göttingen*, 1984
- Watts, J.M., Davies, K.: Rapid frequency analysis of fading radio signals. *J. Geophys. Res.* **65**(8), 2295–2301, 1960

Received November 10, 1985; revised version November 12, 1986

Accepted January 7, 1987